Storage and retrieval of ghost images in hot atomic vapor

Young-Wook Cho,[1,2] **Joo-Eon Oh,**[1] **and Yoon-Ho Kim**[1,*]

[1]*Department of Physics, Pohang University of Science and Technology (POSTECH), Pohang, 790-784, South Korea*

[2]*choyoungwook81@gmail.com*

[*]*yoonho72@gmail.com*

http://qopt.postech.ac.kr

Abstract: Ghost imaging is an imaging technique in which the image of an object is revealed only in the correlation measurement between two beams of light, whereas the individual measurements contain no imaging information. Here, we experimentally demonstrate storage and retrieval of ghost images in hot atomic rubidium vapor. Since ghost imaging requires (quantum or classical) multimode spatial correlation between two beams of light, our experiment shows that the spatially multimode correlation, a second-order correlation property of light, can indeed be preserved during the storage-retrieval process. Our work, thus, opens up new possibilities for quantum and classical two-photon imaging, all-optical image processing, and quantum communication.

OCIS codes: (270.1670) Coherent optical effects; (270.5585) Quantum information and processing; (030.1640) Coherence.

References and links

1. M. Fleischhauer, A. Imamoglu, and J. P. Marangos, "Electromagnetically induced transparency: optics in coherent media," Rev. Mod. Phys. **77**, 633-673 (2005).
2. M. Fleischhauer and M. D. Lukin, "Dark-state polaritons in electromagnetically induced transparency," Phys. Rev. Lett. **84**, 5094-5097 (2000).
3. D. F. Phillips, A. Fleischhauer, A. Mair, R. L. Walsworth, and M. D. Lukin, "Storage of light in atomic vapor," Phys. Rev. Lett. **86**, 783-786 (2001).
4. M. D. Eisaman, A. André, F. Massou, M. Fleischhauer, A. S. Zibrov, and M. D. Lukin, "Electromagnetically induced transparency with tunable single-photon pulses," Nature, **438**, 837–841 (2005).
5. K. Honda, D. Akamatsu, M. Arikawa, Y. Yokoi, K. Akiba, S. Nagatsuka, T. Tanimura, A. Furusawa, and M. Kozuma, "Storage and retrieval of a squeezed vacuum," Phys. Rev. Lett. **100**, 093601 (2008).
6. H. Tanji, S. Ghosh, J. Simon, B. Bloom, and V. Vuletić, "Heralded single-magnon quantum memory for photon polarization states," Phys. Rev. Lett. **103**, 043601 (2009).
7. Y.-W. Cho and Y.-H. Kim, "Atomic vapor quantum memory for a photonic polarization qubit," Opt. Express **18**, 25786 (2010).
8. Y.-W. Cho and Y.-H. Kim, "Storage and retrieval of thermal light in warm atomic vapor," Phys. Rev. A **82**, 033830 (2010).
9. A. L. Alexander, J. J. Longdell, M. J. Sellars, and N. B. Manson, "Photon echoes produced by switching electric fields," Phys. Rev. Lett. **96**, 043602 (2006).
10. M. U. Staudt, S. R. Hastings-Simon, M. Nilsson, M. Afzelius, V. Scarani, R. Ricken, H. Suche, W. Sohler, W. Tittel, and N. Gisin, "Fidelity of an optical memory based on stimulated photon echoes," Phys. Rev. Lett. **98**, 113601 (2007).
11. M. P. Hedges, J. J. Longdell, Y. Li, and M. J. Sellars, "Efficient quantum memory for light," Nature **465**, 1052-1056 (2010).

#161004 - $15.00 USD Received 5 Jan 2012; revised 12 Feb 2012; accepted 13 Feb 2012; published 24 Feb 2012

12. C. Clausen, I. Usmani, F. Bussires, N. Sangouard, M. Afzelius, H. de Riedmatten, and N. Gisin, "Quantum storage of photonic entanglement in a crystal," Nature **469**, 508-511 (2011).
13. M. Hosseini, B. M. Sparkes, G. Campbell, P. K. Lam and B. C. Buchler, "High efficiency coherent optical memory with warm rubidium vapour," Nat. Commun. **2**, 174 (2011).
14. K. F. Reim, J. Nunn, V. O. Lorenz, B. J. Sussman, K. C. Lee, N. K. Langford, D. Jaksch, and I. A. Walmsley, "Towards high-speed optical quantum memories," Nat. Photonics **4**, 218–221 (2010).
15. D. V. Vasilyev, I. V. Sokolov, and E. S. Polzik, "Quantum memory for images: a quantum hologram," Phys. Rev. A. **77**, 020302(R) (2008).
16. P. K. Vudyasetu, R. M. Camacho, and J. C. Howell, "Storage and retrieval of multimode transverse images in hot atomic rubidium vapor," Phys. Rev. Lett. **100**, 123903 (2008).
17. M. Shuker, O. Firstenberg, R. Pugatch, A. Ron, and N. Davison, "Storing images in warm atomic vapor," Phys. Rev. Lett. **100**, 223601 (2008).
18. G. Heinze, A. Rudolf, F. Beil, and T. Halfmann, "Storage of images in atomic coherences in a rare-earth-ion-doped solid," Phys. Rev. A **81**, 011401(R) (2010).
19. T. B. Pittman, Y. H. Shih, D. V. Strekalov, and A. V. Sergienko, "Optical imaging by means of two-photon quantum entanglement," Phys. Rev. A **52**, R3429 (1995).
20. F. Ferri, D. Magatti, A. Gatti, M. Bache, E. Brambilla, and L. A. Lugiato, "High-resolution ghost image and ghost diffraction experiments with thermal light," Phys. Rev. Lett. **94**, 183602 (2005).
21. A. Valencia, G. Scarcelli, M. D'Angelo, and Y. Shih, "Two-photon imaging with thermal light," Phys. Rev. Lett. **94**, 063601 (2005).
22. G. Brida, M. Genovese, and I. R. Berchera, "Experimental realization of sub-shot-noise quantum imaging," Nat. Photonics **4**, 227–230 (2010).
23. R. E. Meyers, K. S. Deacon, and Y. Shih, "Ghost-imaging experiment by measuring reflected photons," Phys. Rev. A **77**, 041801(R) (2008).
24. J. Cheng and S. Han, "Incoherent coincidence imaging and its applicability in X-ray diffraction," Phys. Rev. Lett. **92**, 093903 (2004).
25. P. Clemente, V. Durán, V. Torres-Company, E. Tajahuerce, and J. Lancis, "Optical encryption based on computational ghost imaging," Opt. Lett. **35**, 2391–2393 (2010).
26. V. Boyer, A. M. Marino, R. C. Pooser, and P. D. Lett, "Entangled images from four-wave mixing," Science **321**, 544–547 (2008).
27. G. Scarcelli, V. Berardi, and Y. Shih, "Can two-photon correlation of chaotic light be considered as correlation of intensity fluctuations?," Phys. Rev. Lett. **96**, 063602 (2006).
28. A. Gatti, E. Brambilla, M. Bache, and A. Lugiato, "Correlated imaging, quantum and classical," Phys. Rev. A **70**, 013802 (2004).
29. The cross correlation for the ghost imaging is calculated by the following equation, $G(\vec{r}) = \sum_i^N \Delta\mathbf{I}_i \Delta\mathbf{J}_i(\vec{r})$, where $\Delta\mathbf{I}_i = \mathbf{I}_i - \frac{1}{N}\sum_i^N \mathbf{I}_i$ and $\Delta\mathbf{J}_i(\vec{r}) = \mathbf{J}_i(\vec{r}) - \frac{1}{N}\sum_i^N \mathbf{J}_i(\vec{r})$ are fluctuations of photodetector and CCD output signals, respectively.
30. A delay/pulse generator (SRS, DG535) provides the synchronization pulses for the CCD (JAI, CM-030-GE), the digitizer (NI, PCI-5114), and the two acousto-optic modulators used in the experiment. Each "measurement" is then repeated at 1.5 Hz.
31. K. W. C. Chan, M. N. O'Sullivan, and R. W. Boyd, "Optimization of thermal ghost imaging: high-order correlation vs. background subtraction," Opt. Express **18**, 5562–5573 (2010).
32. K. W. C. Chan, M. N. O'Sullivan, and R. W. Boyd, "High-order thermal ghost imaging," Opt. Lett. **34**, 3343–3345 (2009).
33. B. I. Erkmen and J. H. Shapiro, "Signal-to-noise ratio of Gussian-state ghost imaging," Phys. Rev. A **79**, 023833 (2009).
34. G. Brida, M. V. Chekhova, G. A. Fornaro, M. Genovese, E. D. Lopaeva, and I. Ruo Berchera, "Systematic analysis of signal-to-noise ratio in bipartite ghost imaging with classical and quantum light," Phys. Rev. A **83**, 063807 (2011).
35. F. Ferri, D. Magatti, L. A. Lugiato, and A. Gatti, "Differential ghost imaging," Phys. Rev. Lett. **104**, 253603 (2010).
36. L. Zhao, T. Wang, Y. Xiao, and S. F. Yelin, "Image storage in hot vapors," Phys. Rev. A **77**, 041802(R) (2008).
37. A. Gatti, M. Bache, D. Magatti, E. Brambilla, F. Ferri, and L. A. Lugiato, "Coherent imaging with pseudo-thermal incoherent light," J. of Mod. Opt. **53**, 739–760 (2006).

1. Introduction

Dynamic and reversible storage of the optical field has great potential both in classical (all-optical signal and image processing, etc.) and quantum information (quantum communication, photonic quantum computing, etc.) One promising approach to achieve coherent storage of the optical field is based on electromagnetically-induced transparency (EIT) in which the propaga-

#161004 - $15.00 USD Received 5 Jan 2012; revised 12 Feb 2012; accepted 13 Feb 2012; published 24 Feb 2012

tion of a weak signal field is coherently manipulated by a strong coupling field [1]. Since the quantum state of the signal field is preserved during the storage-retrieval process in the EIT medium [2], the EIT-based light storage facilitates photonic quantum memory [3–8]. In recent years, other schemes for coherent light storage have also become available, including controlled reversible inhomogeneous broadening, atomic frequency comb, gradient echo memory, and off-resonant Raman memory [9–14].

Lately, there have been great interests in expanding the capacity of coherent light storage to spatially multimode fields for storing optical images [15–18]. To date, coherent storage of optical images has been demonstrated only for images imprinted directly on the transverse profile of a laser pulse which is a first-order multimode property of light [16–18]. Then, the question naturally arises: Can a second-order multimode correlation property of light be coherently stored and retrieved? One prominent and useful example of the second-order multimode correlation property of light is the transverse correlation between two beams of light which directly leads to ghost imaging.

Ghost imaging is an imaging technique in which the image of an object is revealed only in the second-order correlation measurement between two beams of light, whereas the individual measurements contain no imaging information [19]. Since quantum (classical) ghost imaging requires spatially multimode quantum (classical) correlation between two beams of light [20, 21], the question is directly related to whether or not spatially multimode (quantum or classical) correlation between beams of light would survive the storage-retrieval process. As the ghost imaging technique has a number of interesting potential applications, including sub-shot noise quantum imaging [22], remote sensing [23], X-ray diffraction imaging [24], and optical encryption [25], the ability to coherently store (quantum or classical) ghost images would significantly advance and bring practicality to these applications. Furthermore, coherent storage of spatially multimode correlation would lead to new applications of entangled images [26].

In this paper, for the first time, we report storage and retrieval of ghost images in hot atomic rubidium vapor. By making use of the thermal ghost imaging scheme [20, 21] and the EIT light storage technique [3], we demonstrate experimentally that the ghost image can still be revealed in the second-order correlation measurement of the retrieved fields. This result establishes clearly that the transverse multimode correlation can in fact survive the storage-retrieval process, enabling potential applications of quantum and classical correlation imaging.

2. Experimental setup

The experimental setup is shown in Fig. 1. Let us first describe the source of correlated twin speckle beams used in the experiment. The transverse correlated twin speckle beams were generated by splitting a pseudo-thermal light beam with a polarizing beam splitter PBS1 [20, 21]. The pseudo-thermal light source was prepared by focusing an external cavity diode laser beam, locked to one of the Rubidium 87 D1 transition lines $5^2S_{1/2}F = 1 \rightarrow 5^2P_{1/2}F' = 2$, at a rotating ground disk (not shown in Fig. 1) [8]. To characterize the temporal properties of the pseudo-thermal light, we measured the second-order temporal coherence of the light by using the Hanbury-Brown–Twiss interferometer. The light reflected at PBS1 was collected at a single-mode fiber connected to a 3dB fiber beam splitter. The two outputs of the fiber beam splitter were connected to single-photon detectors for measuring the second-order temporal correlation function $g^{(2)}(\tau)$ [8]. For thermal light, $g^{(2)}(\tau) = 1 + \exp[-\pi(\tau/\tau_c)^2]$ and the measurement showed clear signature of photon bunching, which is a characteristic of thermal light, with the coherence time of $\tau_c = 7.26 \pm 0.07\ \mu$s .

Let us now describe the experimental setup shown in Fig. 1(a). Ghost imaging makes use of the transverse spatial correlation of the twin speckle beams prepared by splitting the thermal light beam into two with PBS1. The reflected beam at PBS1 (the reference beam; vertically

#161004 - $15.00 USD Received 5 Jan 2012; revised 12 Feb 2012; accepted 13 Feb 2012; published 24 Feb 2012

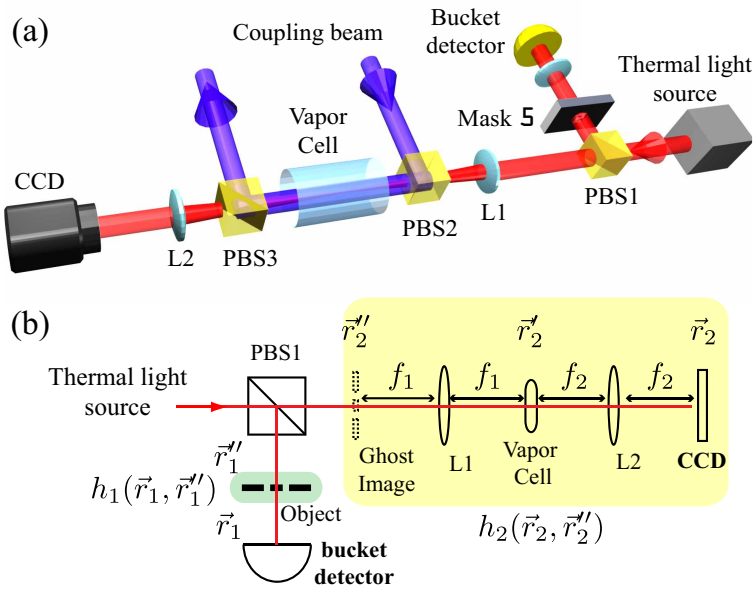

Fig. 1. (a) Two beams that have transverse spatial correlation are prepared by splitting a thermal light beam with a polarizing beam splitter PBS1. One beam (reference) goes through the mask with OCR-a character 5 and is detected by a bucket detector. The other beam (signal) is stored in and retrieved from the EIT medium (Rb vapor cell). Note that neither the bucket detector nor the CCD alone provide any information about the object (mask). The ghost image of the mask is revealed in the correlation measurement between the bucket detector and the CCD. (b) Schematic diagram of the experiment. See text for details.

polarized) goes through the mask (resolution target; Newport RES-1) with OCR-a character 5 and gets detected by a bucket detector. The transmitted beam at PBS1 (the signal beam; horizontally polarized) is stored to and retrieved from the EIT medium (Rubidium vapor cell). The vertically polarized coupling beam, locked to the Rubidium 87 D1 transition line $5^2S_{1/2}F = 2 \rightarrow 5^2P_{1/2}F' = 2$, is spatially and temporally matched with the signal beam inside the vapor cell for preparation and manipulation of the EIT medium. Note that both the bucket detector and the CCD individually do not exhibit any imaging information. The ghost image of the mask is revealed in the correlation measurement between the bucket detector and the CCD.

A more detailed schematic of the experimental setup is shown in Fig. 1(b). At the detection plane (the bucket detector and the CCD), the light field can be written as $E_{out}(\vec{r}_i) = \int d\vec{r}_i'' E_{in}(\vec{r}_i'') h_i(\vec{r}_i,\vec{r}_i'')$, where $\vec{r}_i''$ is the transverse position vector, $E_{in}(\vec{r}_i'')$ refers to the fields at the plane immediately after PBS1, and $h_i(\vec{r}_i,\vec{r}_i'')$ is the impulse response function of each optical system. In the reference beam, an object (Mask with OCR-a character 5) is placed immediately after PBS1. Thus, the impulse response function is given as $h_1(\vec{r}_1,\vec{r}_1'') = T(\vec{r}_1'')\delta(\vec{r}_1 - \vec{r}_1'')$ where $T(\vec{r}_1'')$ is the complex transmission function of the object. In the signal beam, the optical system consists of a $4f$ imaging system and the EIT medium (vapor cell). The impulse response function of the optical system without the EIT medium can be written as $h_2(\vec{r}_2,\vec{r}_2'') = \delta(\vec{r}_2 + m\vec{r}_2'')$, where $m = f_2/f_1$ is the magnification factor. Note that due to the lensless ghost imaging effect [27], the sharp ghost image of the object placed in the reference beam at $\vec{r}_1''$ can be found by correlation measurement of the bucket detector and the CCD placed in the signal beam at the same distance from PBS1 at $\vec{r}_2''$. The ghost image plane $\vec{r}_2''$ is then relayed to $\vec{r}_2$ using the $4f$

#161004 - $15.00 USD Received 5 Jan 2012; revised 12 Feb 2012; accepted 13 Feb 2012; published 24 Feb 2012

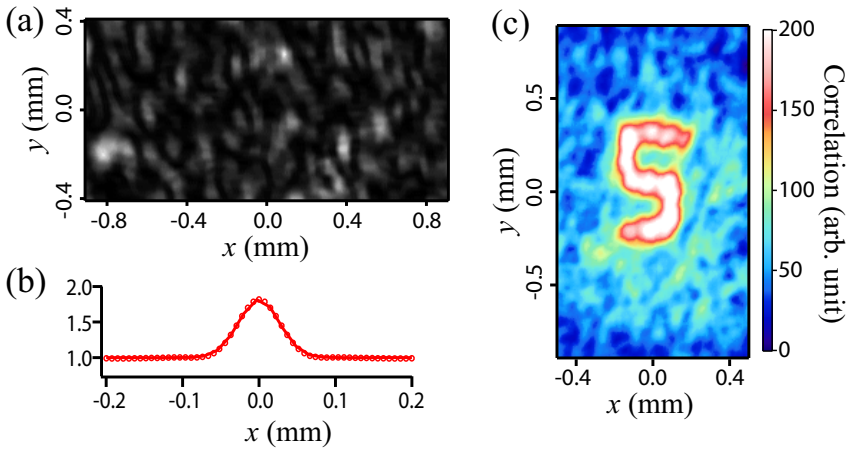

Fig. 2. Reconstruction of the ghost image. (a) A single shot image of the CCD shows the speckle pattern. (b) Normalized spatial intensity autocorrelation measured from the speckle pattern. (c) The reconstructed ghost image, averaged over 5,000 shots. An inverted image of the mask (OCR-a character 5) is revealed.

imaging system with $m = 0.667$

3. Construction of ghost images

The correlation of the intensity fluctuations measured at the two detectors is given as $G(\vec{r}_1,\vec{r}_2) = \langle \Delta I_1(\vec{r}_1)\Delta I_2(\vec{r}_2)\rangle$, where $\langle ...\rangle$ is time averaging and, for thermal light, it becomes [28] $G(\vec{r}_1,\vec{r}_2) \propto |\int d\vec{r}_1'' \int d\vec{r}_2'' h_1^*(\vec{r}_1,\vec{r}_1'')h_2(\vec{r}_2,\vec{r}_2'')\Gamma(\vec{r}_1'',\vec{r}_2'')|^2$, where $\Gamma(\vec{r}_1'',\vec{r}_2'') = \langle E_{in}^*(\vec{r}_1'')E_{in}(\vec{r}_2'')\rangle$ is the mutual spatial correlation function. Assuming that the thermal light is spatially incoherent with a uniform intensity distribution $\Gamma(\vec{r}_1'',\vec{r}_2'') = I_0\delta(\vec{r}_1'' - \vec{r}_2'')$ and this gives rise to $G(\vec{r}_1,\vec{r}_2) \propto |T(\vec{r}_1)|^2 |\delta(\vec{r}_1 + m\vec{r}_2)|^2$. Since the reference beam is detected by a bucket detector which has no spatial resolution, integration of $G(\vec{r}_1,\vec{r}_2)$ over $\vec{r}_1$ is necessary and this yields $\int d\vec{r}_1 G(\vec{r}_1,\vec{r}_2) \propto |T(-m\vec{r}_2)|^2$. Thus, in the absence of the EIT storage medium, we expect to observe an inverted ghost image with the magnification factor of m.

To be able to extract the ghost image from the correlation measurement, the measurement time should be smaller than the coherence time of the light source, $\tau_c = 7.26$ μs. Our CCD, however, has the minimum exposure window of 43 μs. Thus, we shaped the thermal light into a 10 μs square pulse by using an acousto-optic modulator and by delaying the CCD triggering time by 6 μs with respect to the main clock, we are able to achieve an effective 4 μs exposure window. The experimental ghost image is shown in Fig. 2 and, for this measurement, the coupling beam was turned off so that the vapor cell did not act as an EIT medium. As shown in Fig. 2(a), a single shot image from the CCD in the signal beam exhibits a random speckle pattern. The spatial intensity autocorrelation function calculated from this measurement shows a clear signature of the spatial bunching effect, see Fig. 2(b). Note that the the full width at half maximum (FWHM) of the spatial intensity autocorrelation gives the transverse coherence length of the beam, 67.0 ± 0.4 μm, which is related to the resolution of the ghost image [20]. The digitized signal from the bucket detector as well as the CCD output are recorded in a computer. The cross-correlation measurement of the two output signals (photodetector and CCD) [29] are averaged over 5,000 shots to reveal the ghost image of the mask, Fig. 2(c). Note that, as expected, the ghost image is inverted and reduced in size.

#161004 - $15.00 USD Received 5 Jan 2012; revised 12 Feb 2012; accepted 13 Feb 2012; published 24 Feb 2012

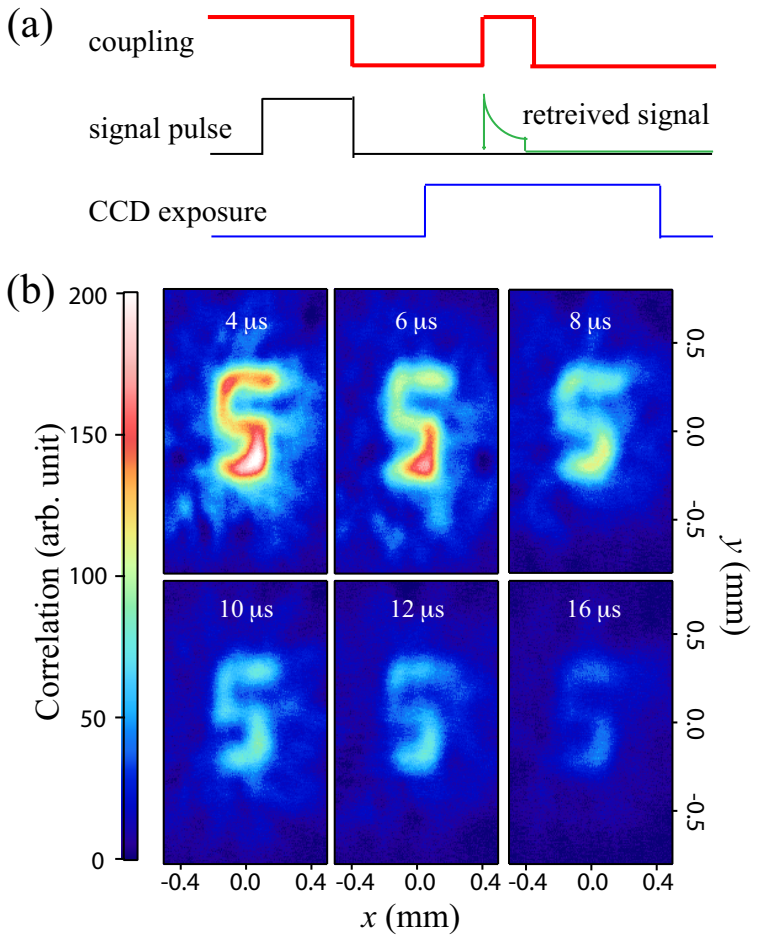

Fig. 3. (a) Synchronized timing sequence for storage and retrieval of ghost images. (b) Ghost image storage and retrieval. The storage time is 4 μs $\sim$ 16 μs. The ghost images are reconstructed from 5,000 shots of bucket detector - CCD correlation measurements.

4. Storage and retrieval of ghost images

Having seen the ghost image, we now move on to discussing storage and retrieval of the ghost image. The 50 mm long natural isotopic abundant Rubidium vapor cell (filled with 49 Torr Ne buffer gas to enhance the storage time by reducing the diffusion velocity of the atoms) is placed at the Fourier plane of the $4f$ imaging system. The vapor cell was heated to $70 \sim 80$ $^{\circ}$C, providing a sufficient rubidium vapor density of approximately 10^{12} cm^{-3}. As discussed earlier, the thermal light source and the coupling beam were locked to $5^2S_{1/2}F = 1$ ($|1\rangle$) $\rightarrow$ $5^2P_{1/2}F' = 2$ ($|3\rangle$) and $5^2S_{1/2}F = 2$ ($|2\rangle$) $\rightarrow$ $5^2P_{1/2}F' = 2$ ($|3\rangle$) transitions of Rubidium 87 D1 line, respectively. To ensure better transmission, both beams are slightly blue-detuned by 60 MHz. The FWHM EIT linewidth of 188 kHz was observed by tuning the frequency of the coupling beam. Note that the bandwidth of the thermal light, $1/\tau_c \approx 138$ kHz, fits within the EIT spectrum. The power and the beam diameter of the signal beam are approximately 250 μW and 2.5 mm, respectively, at the ghost object plane, $\vec{r}_2''$ in Fig. 1(b). The power of the coupling beam is 25 mW with a 5 mm beam diameter.

#161004 - $15.00 USD Received 5 Jan 2012; revised 12 Feb 2012; accepted 13 Feb 2012; published 24 Feb 2012

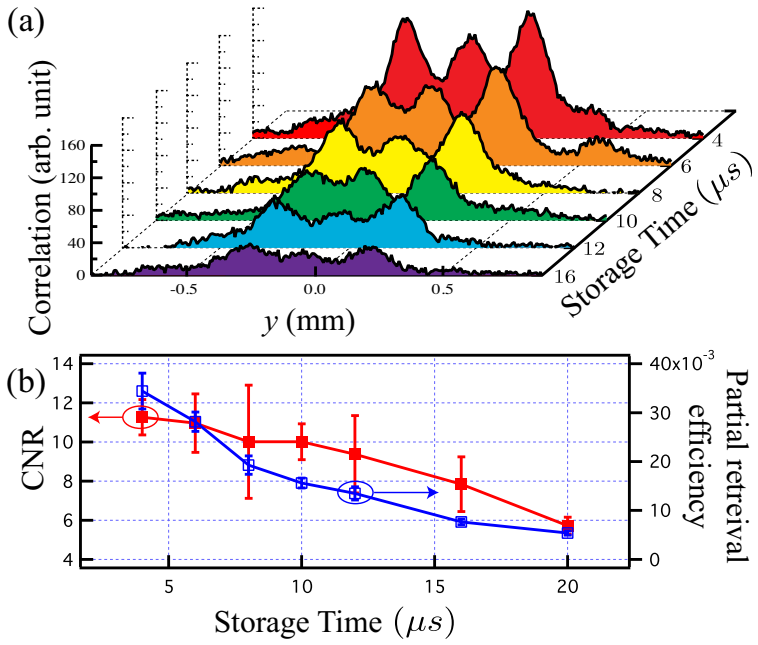

Fig. 4. (a) Vertical cross-sections, at $x = -37$ μm, of the ghost images shown in Fig. 3(b). (b) Contrast-to-Noise Ratio (CNR) of the ghost images and the partial retrieval efficiency with the storage time. The error bars denote statistical one standard deviation errors.

Figure 3(a) shows the synchronized timing sequence employed for storage and retrieval the ghost image [30]. First, the thermal light source is shaped to a 10 μs rectangular pulse as mentioned earlier and the coupling beam is turned on to prepare the EIT medium for storage. After the signal pulse has completely entered the vapor cell, the coupling beam is turned off, storing the signal beam in the EIT medium. After some storage duration (4 μs $\sim$ 20 μs), the coupling beam is temporally turned back on for 4 μs and, during this time, the signal beam stored in the EIT medium is partially retrieved. The CCD is triggered so that the exposure window overlaps only with the retrieved signal.

The ghost images reconstructed from the correlation measurement of the reference beam (with a bucket detector) and the stored signal beam (with a CCD) are shown in Fig. 3(b). The storage time varies between 4 μs to 16 μs and each ghost image is reconstructed from 5,000 shots of such measurements. It is apparent that transverse spatial multimode correlation between the twin speckle beams survives the storage-retrieval process. Also, the reconstructed ghost images are clearly identifiable without broadening by atomic diffusion.

To analyze the effect of storage time on the quality of the ghost image more clearly, we plot the vertical cross-sections of the ghost images in Fig. 4(a). The cross-sectional plots show that the magnitude of the correlation coefficient decays exponentially with the storage time. The visibility(contrast) values calculated from each cross-sectional data set do not vary much. However, the thermal light ghost images have the large background noise. This, then, suggests that the quality of the ghost image is more properly characterized not only with visibility but also with signal-to noise-ratio [31–34]. We will use the contrast-to-noise ratio (CNR) defined in Ref. [31] as the metric for quantifying quality of retrieved ghost images. Figure 4(b) shows the CNR and the partial retrieval efficiency ($\int_{t_s}^{t_s+4\mu s} |E_{out}(t)|^2 dt / \int_{-\infty}^{\infty} |E_{in}(t)|^2 dt$) as a function of storage time. Clearly, the quality of the retrieved ghost images is degraded with longer storage

#161004 - $15.00 USD Received 5 Jan 2012; revised 12 Feb 2012; accepted 13 Feb 2012; published 24 Feb 2012

times and this is mainly due to the fact that, with longer storage times, reduced the retrieval efficiency is reduced. (the reduced intensity decreases both the contrast and the signal-to-noise ratio.) However, as the visibility is not severely degraded with longer storage times, it is possible to increase CNR by taking more measurements [31]. Additionally, computational algorithms can help to increase the ghost imaging CNR and resolution [35].

The effect of storage time on the image quality can be theoretically studied as follows. The signal field $E_{in}(\vec{r}_2'')$ at the ghost object plane is Fourier transformed by the lens (L1) and stored as the coherence between the atomic ground states $|1\rangle$ and $|2\rangle$ [2]. The atomic ground state coherence ρ_{12} evolves according to the diffusion equation

$$\frac{\partial \rho_{12}(\vec{r}_2',t)}{\partial t} = D\left(\frac{\partial^2}{\partial x'^2}+\frac{\partial^2}{\partial y'^2}\right)\rho_{12}(\vec{r}_2',t)-\Gamma\rho_{12}(\vec{r}_2',t),$$

where D and Γ are the diffusion coefficient and the ground state decay rate, respectively. The field at the detection plane is then given as [16, 36] $E_{out}(\vec{r}_2) = E_{in}(-m\vec{r}_2)\exp(-(\beta+\Gamma)t_s)$, where m is the magnification of the $4f$ imaging system, t_s is the storage time, and $\beta = D(2\pi)^2m^2(x^2+y^2)/(\lambda f_1)^2$. Here, f_1 is the focal length of the first lens L1. The retrieved signal field at the CCD plane is then given as $\int d\vec{r}_2'' h_2(\vec{r}_2,\vec{r}_2'')E_{in}(\vec{r}_2'') = E_{in}(-m\vec{r}_2)\exp(-(\beta+\Gamma)t_s)$. The second-order correlation function is therefore given as $G(\vec{r}_1,\vec{r}_2)\propto|T(\vec{r}_1)|^2|\delta(\vec{r}_1+m\vec{r}_2)|^2\exp(-2(\beta+\Gamma)t_s)$. The ghost image is obtained by integrating over $\vec{r}_1$

$$\int d\vec{r}_1 G(\vec{r}_1,\vec{r}_2)\propto|T(-m\vec{r}_2)|^2\exp(-2(\beta+\Gamma)t_s).$$

This result shows that the ghost image can survive the storage-retrieval process while maintaining sharp edges although the overall "brightness" of the ghost image experiences exponential decay. Thus, as mentioned before, CNR of the ghost image can be improved by including more shots of measurements in ghost image reconstruction which is more or less equivalent to making a longer exposure in photography. We note that we could avoid the image degradation due to the atomic diffusion by storing the Fourier transformed image. Zero crossings in the Fourier transformed image is much insensitive to the atomic diffusion due to the destructive interference [16, 36]. (The thermal light ghost imaging is a coherent imaging method although incoherent thermal light source is used. [37])

5. Conclusion

We have demonstrated experimentally storage and retrieval of thermal light ghost images in hot atomic vapor. The results therefore clearly show that transverse spatial multimode correlation can be preserved during the storage-retrieval process. With the recent experimental results on the storage of quantum correlation in a single spatial mode, our result of preservation spatial multimode correlation in the EIT medium strongly implies the possibility to realize the storage of spatially multimode quantum correlation since storage-retrieval process is coherent. We therefore believe that the ghost imaging storage demonstrated in this work will open up important new applications of quantum and classical correlation imaging, all-optical image processing, remote sensing, quantum communication, and quantum information processing in high dimensions.

Acknowledgments

We would like to thank G. Scarcelli and J. Wen for helpful comments. This work was supported by National Research Foundation of Korea (2009-0070668 and 2009-0084473). YWC acknowledges the financial support provided by the NRF (2011-0010895).

#161004 - $15.00 USD Received 5 Jan 2012; revised 12 Feb 2012; accepted 13 Feb 2012; published 24 Feb 2012